

Half-Open Ferrocenes and Ruthenocenes Containing an Edge-Bridged Open Indenyl Ligand

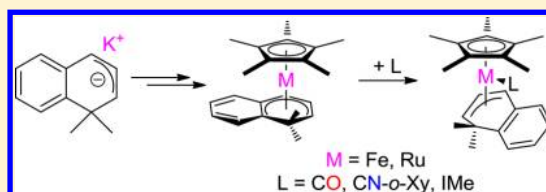
Jeroen Volbeda, Constantin G. Daniliuc, Peter G. Jones, and Matthias Tamm*

Institut für Anorganische und Analytische Chemie, Technische Universität Braunschweig, Hagenring 30, 38106 Braunschweig, Germany

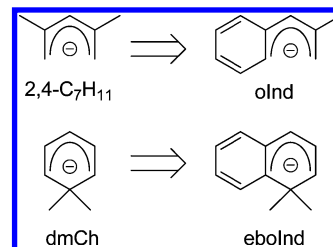
S Supporting Information

ABSTRACT: Potassium 1,1-dimethyl-1,2-dihydronaphthalenide, K(eboInd) (**1**), was synthesized in three steps from 4,4-dimethyl-1-tetralone and used for the synthesis of half-open metallocenes containing an edge-bridged open indenyl ligand (eboInd). Successive treatment of [(THF)FeI₂] with Li(C₅Me₅) and **1** at low temperatures afforded [(η⁵-C₅Me₅)Fe(η⁵-eboInd)] (**2**), whereas [(η⁵-C₅Me₅)Ru(η⁵-eboInd)] (**3**) was synthesized by reaction of **1** with [(C₅Me₅)RuCl]₄. Both compounds

reacted with CO and 2,6-dimethylphenyl isocyanide (CN-*o*-Xy) to form [(η⁵-C₅Me₅)M(η³-eboInd)L] (**4**: M = Fe, L = CO; **5**: M = Ru, L = CO; **6**: M = Fe, L = CN-*o*-Xy; **7**: M = Ru, L = CN-*o*-Xy), in which the eboInd ligand has undergone an η⁵-to-η³ hapticity conversion. In contrast, the N-heterocyclic carbene 1,3,4,5-tetramethylimidazolin-2-ylidene (IMe) only reacted with the ruthenocene derivative **3** to give [(η⁵-C₅Me₅)Ru(η³-eboInd)(IMe)] (**8**). The molecular structures of **2–7** were determined by X-ray diffraction analysis. None of the iron–ruthenium pairs are isotopic.



Scheme 1. Conceptualization of Open Indenyl Ligands from Known Pentadienyl Ligands



INTRODUCTION

Metal–pentadienyl chemistry has received considerable attention over the past few decades, and pentadienyl (“open cyclopentadienyl”, oCp) ligands are well known for their wide range of coordination modes; notably η⁵, η³, and η¹ are accessible.¹ Switching between these coordination modes is easier once one of the π-bonds is less strongly coordinated to the metal atom, as is the case for instance in heteropentadienyl-transition-metal complexes, which are known to undergo a hapticity switch upon addition of an additional ligand under mildly forcing conditions.² Similarly, our group recently employed a phenylmethallyl (“open indenyl”, oInd^{Me}) ligand for the preparation of half-open metallocenes of the type [(η⁵-C₅Me₅)M(η⁵-oInd^{Me})] (M = Fe, Ru), which readily underwent η⁵-to-η³ hapticity interconversion and formed the complexes [(η⁵-C₅Me₅)M(η³-oInd^{Me})L] (M = Fe, Ru with L = CO, PMe₃; M = Ru with L = 2,6-dimethylphenyl isocyanide (CN-*o*-Xy); M = Fe with L = 1,3,4,5-tetramethylimidazolin-2-ylidene (IMe)) upon addition of two-electron donor ligands.³ The oInd^{Me} ligand can be viewed as the indenyl analogue of the widely used 2,4-dimethylpentadienyl (2,4-C₇H₁₁) ligand (Scheme 1), while benzannulation weakens coordination through the endocyclic π-bond and facilitates the switch to the η³-coordination mode by rearomatization of the benzene ring. This could be considered a more extreme example of the indenyl effect,⁴ where the rate increase in ligand exchange is also attributed to a hapticity switch.⁵

An important pentadienyl subclass is formed by so-called edge-bridged open cyclopentadienyls (eboCp), for which 6,6-dimethylcyclohexadienyl (dmCh) is a prominent example. These species have properties in between those of pentadienyl and cyclopentadienyl ligands;⁶ for instance, their reactivity is

such that, unlike pentadienyl ligands, they are able to stabilize group 4 metals in high oxidation states.⁷ Just as eboCp ligands may be considered as more strongly bound ancillary ligands, one should also expect edge-bridged open indenyl (eboInd) ligands to afford less reactive transition metal complexes with a reduced propensity to undergo η⁵-to-η³ hapticity conversion in comparison with their open indenyl (oInd^{Me}) counterparts. Therefore, we were interested in investigating the coordination chemistry of the eboInd ligand, which can be formally derived from the dmCh system by benzannulation (“dimethylbenzocyclohexadienyl”, Scheme 1), and report herein the preparation of the potassium salt K(eboInd) (**1**) and its use for the synthesis of the sandwich complexes [(η⁵-C₅Me₅)M(η⁵-eboInd)] and [(η⁵-C₅Me₅)M(η³-eboInd)L] (M = Fe, L = CO, CN-*o*-Xy; M = Ru, CO, CN-*o*-Xy, IMe).

Special Issue: Ferrocene - Beauty and Function

Received: May 29, 2013

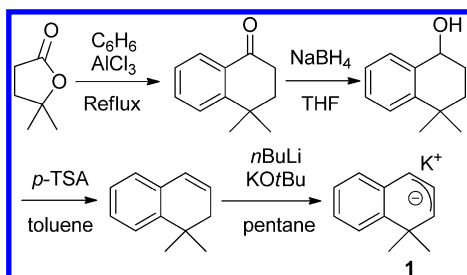


Even though eboInd and transition metal complexes thereof are unknown, it should be noted that several related 1*H*-hydronaphthalene (or more precisely 1,2-dihydro-2-naphthalenyl) complexes are known, in which the (formally) anionic ligand is usually generated in the metal coordination sphere by addition of electrophiles or nucleophiles to a coordinated naphthalene ligand.⁸ As an example, the cymantrene derivative $[(\eta^5\text{-C}_{10}\text{H}_9)\text{Mn}(\text{CO})_3]$ can be accessed either from anionic $[(\eta^4\text{-C}_{10}\text{H}_8)\text{Mn}(\text{CO})_3]^-$ by protonation^{8d,g} or from cationic $[(\eta^6\text{-C}_{10}\text{H}_8)\text{Mn}(\text{CO})_3]^+$ by hydride addition,^{8a,f,h} respectively. Several of these 1,2-dihydro-2-naphthalenyl complexes undergo facile $\eta^5\text{-}\eta^3$ ring slippage,⁹ and this ability was also held responsible for the observation that $[(\eta^5\text{-C}_{10}\text{H}_9)\text{Mn}(\text{CO})_3]$ catalyzes the hydrosilylation of ketones in a far more efficient manner than other cymantrene derivatives.^{9a}

RESULTS AND DISCUSSION

Ligand Synthesis. 4,4-Dimethyl-1-tetralone was synthesized according to a published procedure from ethyl levulinate via γ,γ -dimethylbutyrolactone, which reacted with benzene in the presence of excess aluminum trichloride.¹⁰ The resulting tetralone was reduced to the corresponding alcohol by reaction with NaBH_4 and subsequently dehydrated to afford the 1,1-dimethyl-1,2-dihydronaphthalene.¹¹ Treatment with Schlosser's base¹² afforded the desired potassium 1,1-dimethyl-1,2-dihydronaphthalenide (**1**) as a pyrophoric orange powder (Scheme 2). The ¹H NMR spectrum shows the expected

Scheme 2. Synthesis of the Potassium Salt K(eboInd) (**1**)

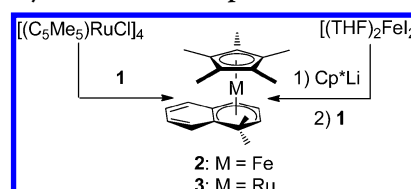


signals for the potassium salt; the bridgehead methyl groups give rise to a singlet at 1.03 ppm, and three characteristic multiplets are found at 5.90 (H2), 4.25 (H3), and 3.39 ppm (H1) for the allylic hydrogen atoms (for the numbering scheme, refer to Chart 1, *vide infra*). These chemical shifts are very similar to those observed for the related 6,6-dimethylcyclohexadienyl potassium salt.¹³

Synthesis and Characterization of Half-Open Metalloenes. In analogy to our previous reports on the coordination chemistry of the open indenyl ligand oInd^{Me}, we aimed at the preparation of the half-open ferrocene and ruthenocene derivatives $[(\eta^5\text{-C}_5\text{Me}_5)\text{M}(\eta^5\text{-eboInd})]$ (M = Fe, **2**; M = Ru, **3**). **2** was obtained by subsequent addition of $(\text{C}_5\text{Me}_5)\text{Li}$ and **1** to a THF solution of $[(\text{THF})_2\text{FeI}_2]$ at -78°C , which afforded a dark green solution. After filtration and removal of the volatiles, a dark green, air-sensitive oil is obtained. According to the ¹H NMR spectrum, the product contains significant amounts of decamethylferrocene (approximately 10%) as well as other impurities, which is in contrast to the previously reported synthesis of the corresponding oInd^{Me} complex,^{3b} which was selectively formed under similar reaction conditions. The product could be purified by column chromatography with pentane over neutral alumina (4 wt %

H_2O) under an argon atmosphere. This gave the fairly pure product in 53% yield as a green oil, which still contained a small amount of decamethylferrocene. An analytically pure sample could be obtained after recrystallization from hexamethyldisiloxane (HMDSO). The half-open ruthenocene **3** was conveniently prepared by reacting $[(\text{C}_5\text{Me}_5)\text{RuCl}]_4$ with **1** in THF at -78°C . After column chromatography with pentane over neutral alumina (4 wt % H_2O) under an argon atmosphere, the product was isolated as an orange, slowly solidifying oil in 69% yield.

Scheme 3. Synthesis of Half-Open Metalloenes



The ¹H NMR spectra of both **2** and **3** provide clear evidence for η^5 -coordination of the eboInd ligand to the metal atoms. The signals found for the hydrogen atoms of the bridgehead methyl groups are particularly diagnostic, since a pronounced high-field shift is observed for the *exo*-methyl groups (Fe: -0.14 ; Ru: 0.30 ppm) relative to the *endo*-methyl groups (Fe: 1.73; Ru: 1.57 ppm). Similar shifts were reported for complexes of the related 6,6-dimethylcyclohexadienyl (dmCh) ligand.^{6a} The signals for the allylic part of the eboInd ligand are found in similar regions for both **2** and **3**, although the signals for the iron compound are spread over a larger area (**2**: H1: 2.07, H2: 3.62, H3: 5.77 ppm; **3**: H1: 2.32, H2: 4.07, H3: 5.54 ppm).

It was previously found that half-open, open, and edge-bridged open ferrocenes are more readily oxidized than ferrocene.^{6c,14} In cyclic voltammetry experiments, the oxidations of **2** and **3** were investigated, showing a quasi-reversible oxidation of **2** at $E_{1/2} = -0.06$ V vs SCE in THF as shown in Figure 1. The cyclic voltammogram of **3** shows a quasi-reversible oxidation at $E_{1/2} = 0.46$ V vs SCE and an irreversible oxidation at $E_p^{\text{ox}} = 0.74$ V vs SCE (see Supporting Information) in THF. For related half-open ruthenocenes bearing either a pentadienyl or a heteropentadienyl ligand, it was found that

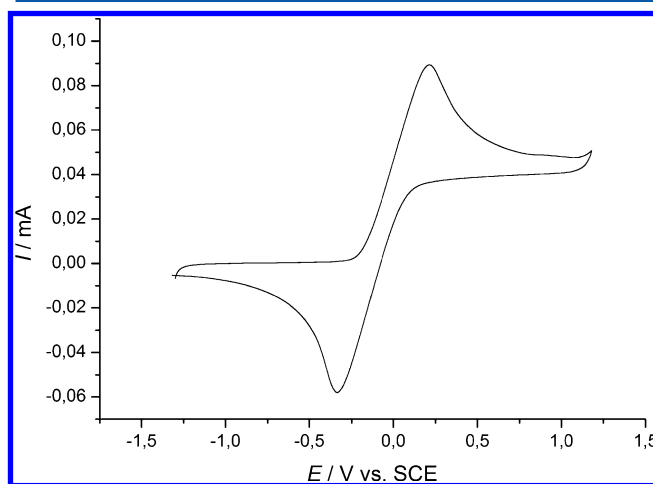


Figure 1. Cyclic voltammogram (CV) for **2**. CV recorded at ambient temperature in THF with 0.1 M $[n\text{-Bu}_4\text{N}][\text{PF}_6]$ supporting electrolyte. Scan rate: 100 mV/s.

oxidation leads to coordination of an acetonitrile solvent molecule concomitant with a change in hapticity.¹⁵

Single crystals of **2** for X-ray diffraction analysis were isolated from a concentrated HMDSO solution at $-30\text{ }^{\circ}\text{C}$, whereas storing the oil obtained after column chromatography overnight at $-30\text{ }^{\circ}\text{C}$ afforded suitable crystals of **3**. Both compounds crystallize in the monoclinic space group $P2_1/c$ (but are not isotypic), and the molecular structures are shown in Figures 2

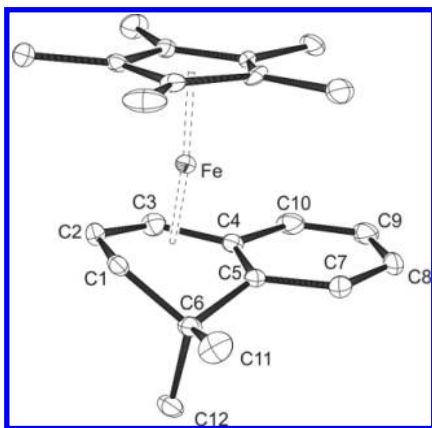


Figure 2. ORTEP drawing of **2** with thermal displacement parameters drawn at 30% probability. The alternative disordered position of the C_5Me_5 ligand and the hydrogen atoms are omitted for clarity. Selected bond lengths [Å] and angles [deg]: Fe–C(C_5Me_5) 1.983(5)–2.105(5), Fe–C1 2.0621(19), Fe–C2 2.0250(19), Fe–C3 2.050(2), Fe–C4 2.1015(19), Fe–C5 2.2074(17), C1–C2 1.401(3), C2–C3 1.415(3), C3–C4 1.429(3), C4–C5 1.439(3), C5–C7 1.424(3), C7–C8 1.368(3), C8–C9 1.411(3), C9–C10 1.347(3), C10–C4 1.437(3); C1–C2–C3 118.61(17), C2–C3–C4 118.63(19), C3–C4–C5 119.08(17).

and **3**, confirming the expected formation of half-open metallocenes. In both cases, the eboInd ligand exhibits a distorted η^5 -coordination mode, with the Fe–C and Ru–C

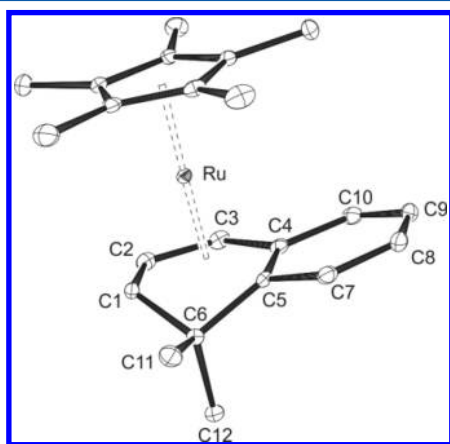


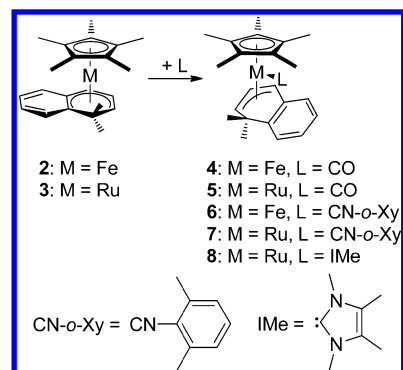
Figure 3. ORTEP drawing of **3** with thermal displacement parameters drawn at 30% probability. The hydrogen atoms are omitted for clarity. Selected bond lengths [Å] and angles [deg]: Ru–C(C_5Me_5) 2.1595(19)–2.203(2), Ru–C1 2.1870(19), Ru–C2 2.169(2), Ru–C3 2.185(2), Ru–C4 2.2295(19), Ru–C5 2.2958(18), C1–C2 1.410(3), C2–C3 1.425(3), C3–C4 1.433(3), C4–C5 1.442(3), C5–C7 1.428(3), C7–C8 1.359(3), C8–C9 1.416(3), C9–C10 1.355(3), C10–C4 1.441(3); C1–C2–C3 118.28(18), C2–C3–C4 118.99(18), C3–C4–C5 118.63(18).

bond lengths ranging from 2.0250(19) Å (Fe–C2) to 2.2074(17) Å (Fe–C5) and from 2.169(2) Å (Ru–C2) to 2.2958(18) Å (Ru–C5), respectively. These distances are slightly shorter than those in the corresponding oInd^{Me} complexes, where the Fe–C and Ru–C bond lengths fall in the ranges 2.055(2)–2.254(2) Å and 2.178(3)–2.312(3) Å.³ The eboInd ligand plane in both complexes approaches the metal atom much more closely than the C_5Me_5 does (1.565 vs 1.646 Å in **2** and 1.713 vs 1.815 Å in **3**), which is similar, albeit less pronounced, to the situation found in the corresponding ferrocene (1.486 vs 1.688 Å) and ruthenocene (1.616 vs 1.821 Å) derivatives bearing the oInd^{Me} ligand.³ These structural differences between the eboInd and oInd^{Me} systems are in agreement with those observed for edge-bridged pentadienyl and pentadienyl systems.⁶

Coordination of a benzene ring to the metal atoms via the C4 and C5 carbon atoms results in bending of the eboInd ligand, as indicated by fold angles between the C4–C5–C7–C8–C9–C10 and C1–C2–C3 planes of 9.8° in **2** and 9.7° in **3**. These angles are smaller than those found in the corresponding oInd^{Me} complexes (11.7° for M = Fe and 14.8° for M = Ru). In addition, benzene coordination leads to a perturbed electron delocalization within the six-membered ring and affords a distinct long–short–long–short–long pattern of the C–C bond lengths along the C5–C7–C8–C9–C10–C4 moieties in both complexes. Overall, the compounds show similar structural features to those observed for related edge-bridged half-open ferrocenes¹⁶ and ruthenocenes.^{17,18}

η^5 -to- η^3 Hapticity Interconversion by Ligand Addition. As was shown in previous studies by our group,³ the half-open indenyl complexes [$(\eta^5\text{-C}_5\text{Me}_5)\text{M}(\eta^5\text{-oInd}^{\text{Me}})$] (M = Fe, Ru) readily switch between the η^5 - and η^3 -coordination modes upon addition of suitable two-electron donor ligands. Naturally, we were interested to see whether the new edge-bridged open indenyl complexes **2** and **3** would show a similar behavior, despite their higher rigidity and potentially greater stability. Upon subjecting toluene solutions of **2** and **3** to an atmosphere of carbon monoxide (Scheme 4), gradual color changes could

Scheme 4. Ligand Addition to the Half-Open Metallocenes **2** and **3**



be observed for both compounds within a couple of days. Whereas the solution of the iron complex **2** changed from green to orange after heating at $70\text{ }^{\circ}\text{C}$ for three days, its ruthenium congener **3** switched more readily, changing from orange to yellow after stirring for two days at room temperature. These observations indicate significantly lower reaction rates than those observed for the oInd^{Me} systems, which show immediate color changes upon exposure to CO

under ambient conditions.³ For comparison, the half-open ferrocene $[(\eta^5\text{-C}_5\text{H}_4\text{tBu})\text{Fe}\{\eta^5\text{-C}_{10}\text{H}_6(\text{OMe})_2\}]$ containing a related 5,8-dimethoxy-1,2-dihydro-2-naphthalenyl ligand adds CO with rearrangement to an η^3 -coordination mode within 5 h at room temperature under 4.5 bar CO pressure.^{8b}

Evaporation of the toluene solutions afforded the carbonyl complexes **4** and **5** as orange and yellow solids, which could be further purified by recrystallization from diethyl ether. Coordination of CO is clearly indicated by ¹³C NMR resonances at 223.5 (**4**) and 209.7 ppm (**5**); the accompanying hapticity switch is particularly well illustrated by the ¹H NMR signals assigned to the hydrogen atoms of the bridgehead methyl groups, which are now observed between ca. 1.5–1.6 ppm for both the *exo*- and *endo*-methyl groups, whereas the signals for the *exo*-CH₃ groups in the parent complexes **2** and **3** were found at significantly higher field (*vide supra*).

Single crystals suitable for X-ray diffraction analysis were obtained by storing concentrated diethyl ether solutions of **4** and **5** at $-30\text{ }^\circ\text{C}$. The molecular structures clearly reveal the eboInd ligand bound in an η^3 -fashion with the additional carbonyl ligand coordinating toward the open edge of the allyl ligand, which corresponds to an *exo*-conformation.¹⁹ The metal–CO bond lengths of 1.746(3) Å (Fe–C23) and 1.8650(16) Å (Ru–C23) are comparable to those found in similar CO adducts of cyclopentadienyl-allyl metal complexes,^{20,21} and they are nearly identical to the bond lengths previously established for $[(\eta^5\text{-C}_5\text{Me}_5)\text{Fe}(\eta^3\text{-oInd}^{\text{Me}})(\text{CO})]$ (1.7464(14) Å)^{3b} and $[(\eta^5\text{-C}_5\text{Me}_5)\text{Ru}(\eta^3\text{-oInd}^{\text{Me}})(\text{CO})]$ (1.855(2) Å).^{3a} As expected, η^5 -to- η^3 hapticity interconversion goes along with a significantly stronger folding of the eboInd ligand with an increase of the angle between the allyl (C1–C2–C3) and benzene (C4–C5–C7–C8–C9–C10) planes from 9.8° and 9.7° in **2** and **3** to 36.2° and 31.5° in **4** and **5**, respectively. Additionally the bond length alteration of the benzene ring observed in **2** and **3** is not present in complexes **4** and **5**.

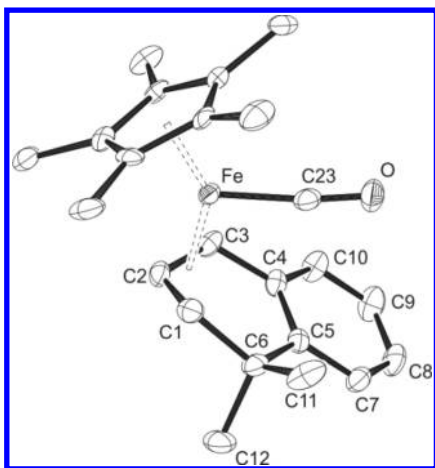


Figure 4. ORTEP drawing of **4** with thermal displacement parameters drawn at 30% probability. The alternative disordered positions of the C₅Me₅ ligand and hydrogen atoms are omitted for clarity. Selected bond lengths [Å] and angles [deg]: Fe–C(C₅Me₅) 2.088(6)–2.1249(7), Fe–C1 2.104(3), Fe–C2 1.984(3), Fe–C3 2.122(3), Fe–C23 1.746(3), C23–O 1.157(3), C1–C2 1.400(4), C2–C3 1.411(4), C3–C4 1.471(4), C4–C5 1.409(4), C5–C7 1.391(4), C7–C8 1.393(4), C8–C9 1.375(4), C9–C10 1.384(4), C10–C4 1.396(4); O–C23–Fe 173.3(2), C1–C2–C3 114.8(3), C2–C3–C4 118.3(3), C3–C4–C5 119.9(2).

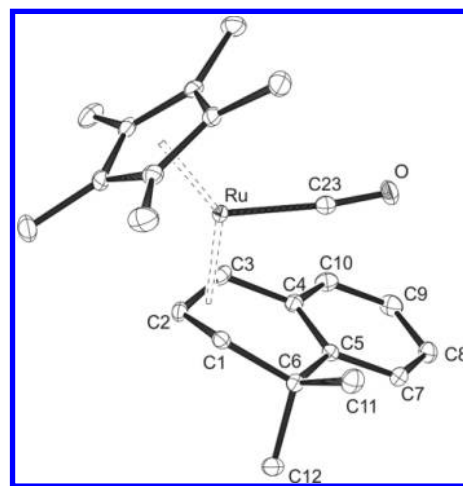


Figure 5. ORTEP drawing of **5** with thermal displacement parameters drawn at 30% probability. The hydrogen atoms are omitted for clarity. Selected bond lengths [Å] and angles [deg]: Ru–C(C₅Me₅) 2.2079(14)–2.2476(14), Ru–C1 2.2149(14), Ru–C2 2.1176(14), Ru–C3 2.2511(15), Ru–C23 1.8650(16), C23–O 1.1544(19), C1–C2 1.417(2), C2–C3 1.420(2), C3–C4 1.479(2), C4–C5 1.410(2), C5–C7 1.392(2), C7–C8 1.390(2), C8–C9 1.383(2), C9–C10 1.388(2), C10–C4 1.398(2); Ru–C23–O 173.54(13), C1–C2–C3 115.34(13), C2–C3–C4 117.93(13), C3–C4–C5 120.25(13).

Addition of 2,6-dimethylphenyl isocyanide to **2** and **3** resulted in similar color changes. Again, compound **2** required heating at $70\text{ }^\circ\text{C}$ for three days to achieve full conversion, whereas compound **3** switched at room temperature over the course of two days. The changes in the NMR spectra of the resulting isocyanide complexes **6** and **7** were analogous to those observed for compounds **4** and **5**, and again, the resonances of the bridgehead methyl groups are most notably affected by switching from a η^5 - to a η^3 -coordination mode (*vide supra*). The CN resonance in **6** is found at 197.6 ppm, whereas the corresponding signal could not be resolved for **7**. Single crystals of **6** and **7** suitable for X-ray diffraction analysis were grown from saturated diethyl ether solutions at $-30\text{ }^\circ\text{C}$. The molecular structures are very similar to those established for **4** and **5**, with the eboInd ligand bound in an η^3 -fashion and adopting an *exo*-conformation relative to the isocyanide ligand (Figures 6 and 7). The metal to isocyanide bond lengths are 1.790(5) Å (Fe–C23) and 1.9044(13) Å (Ru–C23), with the latter value being similar to the distance found for $[(\eta^5\text{-C}_5\text{Me}_5)\text{Ru}(\eta^3\text{-oInd}^{\text{Me}})(\text{CN-}o\text{-Xy})]$ (1.8943(17) Å).^{3a,22}

Addition of the N-heterocyclic carbene 1,3,4,5-tetramethylimidazol-2-ylidene (IMe) proved to be more difficult, and indeed, no reaction with **2** was observed even upon heating for a prolonged period of time, eventually resulting in the decomposition of the starting material. This could be due to the small size of the iron atom, not offering sufficient space for the addition of the carbene ligand. The ruthenium complex **3**, however, was capable of accommodating the carbene, and the carbene complex **8** was isolated as a yellow solid after heating at $60\text{ }^\circ\text{C}$ for three days. The ¹H NMR spectrum of **8** clearly shows the expected signal shifts for the eboInd ligand binding in an η^3 -fashion, although the shifts of signals assigned to the bridgehead methyl groups are not quite as pronounced as those observed for the previous allyl-ruthenium species **5** and **7**. The carbene carbon signal is found at 194.1 ppm in the ¹³C NMR spectrum, and it is worth mentioning that, apart from this resonance, the carbene fragment gives rise to a duplicate set of ¹H and ¹³C

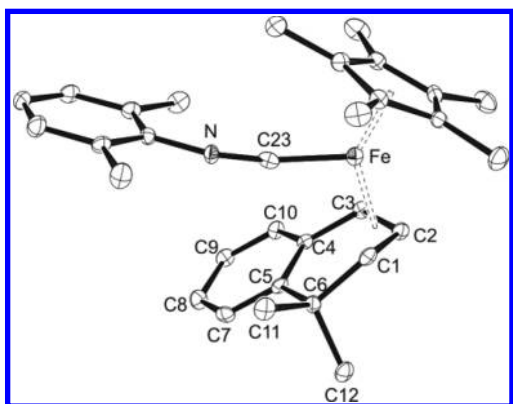


Figure 6. ORTEP drawing of **6** with thermal displacement parameters drawn at 30% probability. The hydrogen atoms are omitted for clarity. Selected bond lengths [Å] and angles [deg]: Fe–C(C₅Me₅) 2.084(5)–2.119(5), Fe–C1 2.110(5), Fe–C2 1.993(5), Fe–C3 2.146(5), Fe–C23 1.790(5), C23–N 1.194, C1–C2 1.418(7), C2–C3 1.404(7), C3–C4 1.457(7), C4–C5 1.409(7), C5–C7 1.384(7), C7–C8 1.390(7), C8–C9 1.399(7), C9–C10 1.384(7), C10–C4 1.400(7); Fe–C23–N 170.9(5), C1–C2–C3 115.3(5), C2–C3–C4 118.7(5), C3–C4–C5 120.7(5).

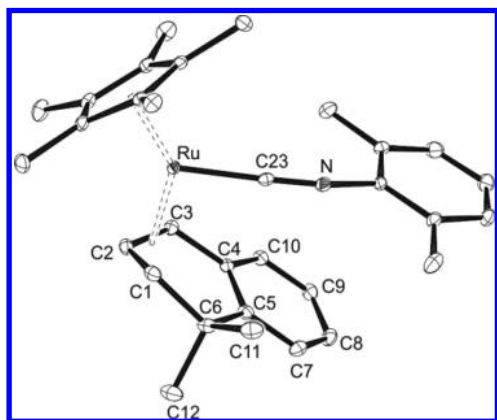


Figure 7. ORTEP drawing of **7** with thermal displacement parameters drawn at 30% probability. The hydrogen atoms are omitted for clarity. Selected bond lengths [Å] and angles [deg]: Ru–C(C₅Me₅) 2.2153(12)–2.2483(12), Ru–C1 2.2182(13), Ru–C2 2.0969(13), Ru–C3 2.2309(12), Ru–C23 1.9044(13), C23–N 1.1828(16), C1–C2 1.420(2), C2–C3 1.4216(18), C3–C4 1.4731(17), C4–C5 1.4096(18), C5–C7 1.3924(18), C7–C8 1.393(2), C8–C9 1.383(2), C9–C10 1.3874(18), C10–C4 1.4007(17); Ru–C23–N 177.97(11), C1–C2–C3 114.71(11), C2–C3–C4 117.88(12), C3–C4–C5 120.70(11).

NMR signals, indicating hindered rotation around the ruthenium–carbene bond at room temperature on the NMR time scale. Finally it should be noted that neither **2** nor **3** reacted with PMe₃, even at elevated temperatures. Apparently, the metal atoms in **2** and **3** are quite efficiently shielded by the bulky C₅Me₅ and eboInd ligands, so that only rod-like or flat molecules readily coordinate and induce switching of the eboInd ligand.

CONCLUSIONS

Potassium 1,1-dimethyl-1,2-dihydronaphthalenide, K(eboInd) (**1**), provides convenient access to half-open metallocenes containing a novel edge-bridged open indenyl ligand. The isolation and structural characterization of the sandwich complexes [(η⁵-C₅Me₅)M(η⁵-eboInd)] (**2**, M = Fe; **3**, M =

Ru) provides evidence for the ability of the eboInd ligand to coordinate to transition metals in an η⁵-fashion, despite the presumably weak π-interaction with the annelated benzene ring. The presence of this weaker bond allows these half-open metallocenes to change their hapticity upon addition of a two-electron donor ligand and to switch readily from an η⁵- to an η³-coordination mode. However, these switches were significantly slower than previously observed for the unbridged open indenyl (oInd^{Me}) system, and this lower reactivity is probably associated with the greater rigidity of the eboInd ligand.

EXPERIMENTAL SECTION

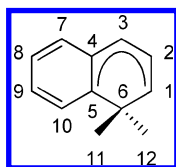
All synthetic and spectroscopic manipulations were carried out under an atmosphere of purified nitrogen, either in a Schlenk apparatus or in a glovebox. Solvents were dried and deoxygenated either by distillation under a nitrogen atmosphere from sodium benzophenone ketyl (THF) or by an MBraun GmbH solvent purification system (all other solvents). NMR spectra were obtained on a Bruker DRX 400 or a Bruker Avance III 400 spectrometer at 400 or 300 MHz (¹H) and 101 or 75 MHz (¹³C). The residual solvent signal was used as a chemical shift reference (δ_H = 7.16 ppm for C₆D₆, δ_H = 1.72, 3.58 ppm for [D₈]THF) for the ¹H NMR spectra and the solvent signal (δ_C = 128.04 ppm for C₆D₆, δ_H = 25.31, 67.21 ppm for [D₈]THF) for the ¹³C NMR spectra. The number of protons attached to each carbon was determined by ¹³C-DEPT135 experiments. If required, signal assignment was achieved by two-dimensional H,H-COSY, H,H-NOESY, H,C-HSQC, and H,C-HMBC NMR spectra. They were recorded using standard Bruker pulse programs; sweep widths, digital resolution, and pulse delays were optimized for the samples under investigation. Mixing times of 1000 and 2000 ms were used for the H,H-NOESY experiments. A Bruker Vertex 70 spectrometer was used for recording IR spectra. Elemental analyses were performed by combustion and gas chromatographic analysis with an Elementar VarioMICRO instrument. Cyclic voltammograms were recorded on a Metrohm μAutolab Type III potentiostat/galvanostat in a THF solution containing 0.1 M [n-Bu₄N][PF₆] as supporting electrolyte; 99.9% platinum wires (φ 0.6 mm, Chempur) were used as working and counter electrode, and the potentials were measured against a 99.9% silver wire (φ 0.6 mm, Chempur). Redox potentials were calculated using the formula ΔE_{1/2} = 1/2(E_p^{ox} + E_p^{red}), where E_p^{ox} and E_p^{red} are peak potentials. Ferrocene was used as a standard for the measurement of **2**. The couple [(η⁵-C₅H₅)₂Fe]⁺/[(η⁵-C₅H₅)₂Fe] displayed a reversible cyclic voltammetric trace with a redox potential ΔE_{1/2} = +0.56 V (in THF) under these conditions.²³ Cobaltocene was used as a standard for **3**, which was itself referenced to ferrocene. The couple [(η⁵-C₅H₅)₂Co]⁺/[(η⁵-C₅H₅)₂Co] displayed a reversible cyclic voltammetric trace with a redox potential ΔE_{1/2} = –0.82 V (in THF) under the chosen measuring conditions. 4,4-Dimethyl-1-tetralone,¹⁰ 1,1-dimethyl-1,2-dihydronaphthalene,¹¹ [Fe₂(thf)₂],²⁴ Li(C₅Me₅),²⁵ and [(C₅Me₅)RuCl]₄²⁶ were prepared according to the literature; all other reagents were obtained commercially and used as received.

X-ray Diffraction Studies. Data were recorded at 100 K on Oxford Diffraction diffractometers using monochromated Mo Kα or mirror-focused Cu Kα radiation (Table 1). The structures were refined anisotropically using the SHELXL-97 program.²⁷ Hydrogen atoms were either (i) located and refined isotropically (H1, H2, H3 for all structures); (ii) included as idealized methyl groups allowed to rotate, but not tip; or (iii) placed geometrically and allowed to ride on their attached carbon atoms. *Special features:* In the iron complexes **2** and **4**, the C₅Me₅ ligand was disordered over two positions. Appropriate restraints and constraints were used to ensure stability of refinement (for details see the Supporting Information). Data for **6** were weak, and the *R* values are correspondingly poor, but the structure serves as proof of the nature of **6**. Complete data have been deposited at the Cambridge Crystallographic Data Centre under the numbers CCDC 941708 (**2**), 941709 (**3**), 941710 (**4**), 941711 (**5**), 941712 (**6**), and 941713 (**7**). These data can be obtained free of charge from www.ccdc.cam.ac.uk/data_request/cif.

Table 1. Crystallographic Data

	2	3	4	5	6	7
empirical formula	C ₂₂ H ₂₈ Fe	C ₂₂ H ₂₈ Ru	C ₂₃ H ₂₈ FeO	C ₂₃ H ₂₈ ORu	C ₃₁ H ₃₇ FeN	C ₃₁ H ₃₇ NRu
fw	348.29	393.51	376.30	421.52	479.47	524.69
temperature (K)	100(2)	100(2)	100(2)	100(2)	100(2)	100(2)
wavelength λ (Å)	0.71073	0.71073	0.71073	1.54184	0.71073	0.71073
cryst syst	monoclinic	monoclinic	triclinic	monoclinic	triclinic	triclinic
space group	P2 ₁ /c	P2 ₁ /c	P $\bar{1}$	P2 ₁ /n	P $\bar{1}$	P $\bar{1}$
a [Å]	8.1835(4)	13.6723(4)	8.2042(8)	8.1412(2)	8.5368(8)	8.49475(18)
b [Å]	24.1385(12)	8.5436(2)	10.1965(8)	18.4127(2)	10.486(2)	11.27251(18)
c [Å]	9.9365(6)	16.0804(4)	13.3248(12)	13.4624(2)	15.658(3)	14.7874(4)
α [deg]	90	90	108.566(8)	90	79.902(18)	92.387(2)
β [deg]	112.222(6)	103.142(2)	98.077(8)	98.800(2)	85.608(12)	103.370(2)
γ [deg]	90	90	108.480(8)	90	66.907(14)	109.317(2)
volume [Å ³]	1817.04(17)	1829.17(8)	965.37(15)	1994.28(6)	1269.3(4)	1289.25(5)
Z	4	4	2	4	2	2
reflns collected	46 155	77 440	33 473	33 698	39 518	62 483
independent reflns	4004 [R _{int} = 0.0580]	4193 [R _{int} = 0.0472]	3966 [R _{int} = 0.1060]	4075 [R _{int} = 0.0291]	4486 [R _{int} = 0.1631]	7416 [R _{int} = 0.0319]
goodness of fit on F ²	1.025	1.097	1.059	1.060	1.099	1.074
ρ _{calcd} [g cm ⁻³]	1.273	1.429	1.295	1.404	1.254	1.352
μ [mm ⁻¹]	0.828	0.855	0.788	6.396	0.613	0.627
R(F _o ²), [I > 2σ(I)]	0.0356	0.0246	0.0523	0.0182	0.0823	0.0214
R _w (F _o ²)	0.0851	0.0581	0.1005	0.0470	0.1981	0.0543
Δρ [e Å ⁻³]	0.810/−0.329	1.739/−0.429	0.551/−0.385	0.381/−0.427	1.159/−0.472	0.540/−0.393

Chart 1. Numbering Scheme for the Assignment of NMR Resonances to the eboInd Fragment



Potassium 1,1-Dimethyl-1,2-dihydronaphthalenide (KeboInd) (1). To a suspension of 1.2 g of potassium *tert*-butoxide (10.7 mmol) in pentane was added 1.7 g of 1,1-dimethyl-1,2-dihydronaphthalene (10.7 mmol). The mixture was stirred and cooled to -78 °C. Then 4.8 mL of *n*-butyllithium (2.5 M in hexane, 12 mmol) was added slowly by syringe. The mixture was allowed to warm to room temperature while stirring overnight. The orange precipitate thus formed on a frit and washed three times with 20 mL of pentane. After drying *in vacuo* 1.9 g (9.7 mmol, 90% yield) of orange pyrophoric **1** was obtained. ¹H NMR (400 MHz; [D₈]THF): δ 6.74 (dd, 1H, *J*_{HH} 0.9, 7.5 Hz, H7), 6.42 (dt, 1H, *J*_{HH} 1.4, 7.5 Hz, H9), 6.22 (dd, 1H, *J*_{HH} 1.4, 8.0 Hz, H10), 5.95 (dt, 1H, *J*_{HH} 1.3, 7.1 Hz, H8), 5.90 (dd, 1H, *J*_{HH} 6.5, 8.0 Hz, H2), 4.25 (d, 1H, *J*_{HH} 6.5 Hz, H3), 3.39 (d, 1H, *J*_{HH} 8.0 Hz, H1), 1.03 (s, 6H, H11) ppm. ¹³C NMR (100 MHz; [D₈]THF): δ 141.8 (C4), 128.0 (C2), 124.9 (C5), 124.8 (C9), 124.6 (C7), 116.6 (C10), 110.9 (C8), 92.1 (C1), 79.1 (C3), 36.7 (C6), 30.3 (C11) ppm. The extremely air-sensitive nature of the product made it impossible to obtain an accurate elemental analysis.

[(η⁵-C₅Me₅)Fe(η⁵-eboInd)] (2). A dark purple solution of 454 mg (1.0 mmol) of [(THF)₂FeI₂] in 10 mL of THF was cooled to -78 °C. A suspension of 142 mg (1.0 mmol) of [Li(C₅Me₅)] in 10 mL of THF was added by syringe. After stirring for 10 min at -78 °C a yellow solution was obtained. To this was added slowly by syringe a solution of 196 mg (1.0 mmol) of K(eboInd) **1** in 10 mL of THF. After stirring overnight and allowing the mixture to slowly reach room temperature, a green solution was obtained. After removing the solvent *in vacuo* the green residue was extracted three times with 20 mL of pentane. The pentane was removed *in vacuo*, and the resulting green oil was further purified by column chromatography under an argon atmosphere over neutral alumina (4 wt % H₂O) with pentane. The product was obtained as a green oil (183 mg, 0.53 mmol, 53% yield). Single crystals suitable for X-ray diffraction analysis could be obtained by storing a

concentrated solution of **2** in HMDSO at -30 °C for several weeks. ¹H NMR (400 MHz; C₆D₆): δ 7.20 (d, *J*_{HH} 8.6 Hz, 1H, H10), 6.94–6.78 (m, 3H, H7, 8, 9), 5.77 (d, *J*_{HH} 5.2 Hz, 1H, H3), 3.62 (t, *J*_{HH} 5.9 Hz, 1H, H2), 2.07 (d, *J*_{HH} 6.4 Hz, 1H, H1), 1.73 (s, 3H, H12), 1.42 (s, 15H, C₅Me₅), −0.14 (s, 3H, H11) ppm. ¹³C NMR (100 MHz; C₆D₆): δ 133.6 (phenyl), 127.5 (C10), 125.6 (phenyl), 122.5 (phenyl), 97.7 (C4), 83.3 (C2), 80.1 (C₅Me₅), 75.9 (C3), 63.9 (C5), 44.2 (C1), 35.4 (C6), 33.9 (C11), 27.4 (C12), 9.8 (C₅Me₅) ppm. Anal. Calcd for C₂₂H₂₈Fe: C, 75.86; H, 8.10. Found: C, 75.19; H, 7.88.

[(η⁵-C₅Me₅)Ru(η⁵-eboInd)] (3). To a suspension of 271.9 mg (0.25 mmol) of [(C₅Me₅)RuCl]₄ in 10 mL of THF at -78 °C was slowly added by syringe a solution of 196.3 mg (1 mmol) of **1** in 10 mL of THF. After removing the cooling bath and stirring overnight a dark red suspension was obtained. The solvent was removed *in vacuo*, and the residue extracted with 20 mL of pentane followed by another 10 mL of pentane. After removing the solvent *in vacuo* a dark red oil was obtained. Column chromatography under argon over neutral alumina (4 wt % H₂O) with pentane gave after removal of the solvent *in vacuo* 272.6 mg (0.69 mmol, 69%) of a bright orange oil, which slowly crystallized at room temperature. ¹H NMR (400 MHz; C₆D₆): δ 6.84–6.70 (m, 4H, H7, 8, 9, 10), 5.54 (d, *J*_{HH} 4.8 Hz, 1H, H3), 4.06 (dd, *J*_{HH} 4.8, 6.2 Hz, 1H, H2), 2.32 (dd, *J*_{HH} 0.9, 6.2 Hz, 1H, H1), 1.57 (s, 3H, H12), 1.50 (s, 15H, C₅Me₅), 0.30 (s, 3H, H11) ppm. ¹³C NMR (100 MHz; C₆D₆): δ 131.8 (C7), 125.5 (C10), 124.1 (C8), 120.8 (C9), 98.0 (C4), 85.0 (C₅Me₅), 81.6 (C2), 76.0 (C3), 67.7 (C5), 45.4 (C1), 38.9 (C6), 35.2 (C11), 27.7 (C12), 10.3 (C₅Me₅) ppm. Anal. Calcd for C₂₂H₂₈Ru: C, 67.15; H, 7.17. Found: C, 67.33; H, 7.17.

[(η⁵-C₅Me₅)Fe(η³-eboInd)(CO)] (4). CO gas was passed through a solution of 50 mg (0.14 mmol) of **2** in 20 mL of toluene for 5 min. The closed vessel was stirred at 70 °C for 3 d. This resulted in a color change from green to orange. After removing the solvent *in vacuo* the orange solid was dissolved in Et₂O. Upon concentrating the solution and storing at -30 °C overnight 29 mg (0.08 mmol, 55%) of orange crystals was obtained. ¹H NMR (400 MHz; C₆D₆): δ 7.00 (d, *J*_{HH} 6.8 Hz, 1H, H7), 6.90 (d, *J*_{HH} 6.6 Hz, H10), 6.87 (dt, 2.3, 7.2 *J*_{HH} Hz, 1H, H8), 6.84 (dt, *J*_{HH} 1.8, 7.2 Hz, 1H, H9), 3.91 (t, *J*_{HH} 5.8 Hz, 1H, H2), 3.89 (d, *J*_{HH} 2.7 Hz, 1H, H3), 3.32 (dd, *J*_{HH} 2.9, 5.8 Hz, 1H, H1), 1.55 (s, 3H, CMe₂), 1.49 (s, 3H, CMe₂), 1.46 (s, 15H, C₅Me₅) ppm. ¹³C NMR (100 MHz; C₆D₆): δ 223.5 (CO), 143.9 (C4), 140.2 (C5), 126.0 (C10), 125.9 (C8), 124.2 (C7,9), 89.0 (C₅Me₅), 76.6 (C2), 69.4 (C1), 58.2 (C3), 40.1 (C6), 38.3 (CMe₂), 30.2 (CMe₂), 9.7 (C₅Me₅)

ppm. Anal. Calcd for $C_{23}H_{28}FeO$: C, 73.41; H, 7.50. Found: C, 73.53; H, 7.54. IR (ATR): $\nu(\text{CO}/\text{cm}^{-1}) = 1918$.

$[(\eta^5\text{-C}_5\text{Me}_5)\text{Ru}(\eta^3\text{-ebolnd})(\text{CO})]$ (5). CO gas was passed through a solution of 50 mg (0.13 mmol) of **3** in 20 mL of toluene for 5 min. After this the closed vessel was stirred at room temperature for 2 d, after which a color change from orange to yellow had occurred. After removing the solvent *in vacuo* the yellow solid was dissolved in diethyl ether. After concentrating the solution and storing at -30°C overnight 29 mg (0.07 mmol, 54%) of yellow crystals was obtained. ^1H NMR (400 MHz; C_6D_6): δ 7.08 (dd, J_{HH} 1.6, 7.2 Hz, 1H, H10), 7.04 (dd, J_{HH} 1.7, 7.2 Hz, 1H, H7), 6.92 (dt, J_{HH} 1.8, 7.3 Hz, 1H, H9), 6.87 (dt, J_{HH} 1.6, 7.3 Hz, 1H, H8), 4.34 (dd, J_{HH} 2.0, 5.2 Hz, 1H, H3), 3.36 (d, J_{HH} 5.2 Hz, 1H, H1), 3.35 (dt, J_{HH} 2.1, 6.9 Hz, 1H, H2), 1.62 (s, 3H, CMe_2), 1.59 (s, 3H, CMe_2), 1.57 (s, 15H, C_5Me_5) ppm. ^{13}C NMR (100 MHz; C_6D_6): δ 209.7 (CO), 144.0 (C4), 140.3 (C5), 126.0 (C7), 125.8 (C9), 124.3 (C8, 10), 93.1 (C_5Me_5), 73.4 (C1), 67.8 (C2), 56.2 (C3), 40.2 (C6), 38.0 (CMe_2), 31.1 (CMe_2), 10.1 (C_5Me_5) ppm. Anal. Calcd for $C_{23}H_{28}\text{RuO}$: C, 65.53; H, 6.70. Found: C, 65.48; H, 6.66. IR (ATR): $\nu(\text{CO}/\text{cm}^{-1}) = 1922$.

$[(\eta^5\text{-C}_5\text{Me}_5)\text{Fe}(\eta^3\text{-ebolnd})(\text{CN-o-Xy})]$ (6). A 44.6 mg (0.34 mmol) amount of 2,6-dimethylphenyl isocyanide was added to a solution of 120 mg (0.34 mmol) of **2** in 20 mL of toluene. The solution was heated at 70°C for 3 d, resulting in an orange solution. After removal of the solvent *in vacuo* the compound was obtained as an orange solid, which was recrystallized by cooling a concentrated Et_2O solution to -30°C overnight. This gave **6** as an orange crystalline solid (72 mg, 0.15 mmol, 44% yield). ^1H NMR (400 MHz; C_6D_6): δ 6.89 (dd, J_{HH} 1.5, 7.5 Hz, 1H, H10), 6.80–6.70 (m, 3H, phenyl), 6.66 (d, J_{HH} 7.6 Hz, 1H, H7), 6.61 (dt, J_{HH} 1.4, 7.4 Hz, 1H, H9), 6.44 (dt, J_{HH} 1.4, 7.4 Hz, 1H, H8), 4.13 (t, J_{HH} 6.4 Hz, 1H, H2), 3.88 (dd, J_{HH} 1.4, 6.0 Hz, 1H, H3), 3.34 (dd, J_{HH} 1.4, 7.0 Hz, 1H, H1), 2.30 (s, 6H, $\text{C}_6\text{H}_4\text{-o-Me}_2$), 1.58 (s, 6H, CMe_2), 1.57 (s, 15H, C_5Me_5) ppm. ^{13}C NMR (100 MHz; C_6D_6): δ 197.6 (oXyNC), 145.3 (C4), 140.8 (C5), 134.6 (*ipso*-phenyl), 132.0 (*ipso*-C-NC), 127.7 (phenyl), 125.3 (phenyl), 125.0 (C7), 124.9 (C9), 124.3 (C10), 122.7 (C8), 87.2 (C_5Me_5), 75.6 (C2), 66.4 (C1), 55.5 (C3), 40.0 (C6), 38.9 (CMe_2), 30.1 (CMe_2), 19.5 ($\text{C}_6\text{H}_4\text{-o-Me}_2$), 10.0 (C_5Me_5) ppm. Anal. Calcd for $\text{C}_{31}\text{H}_{37}\text{FeN}$: C, 77.65; H, 7.78; N, 2.92. Found: C, 77.47; H, 7.73; N, 2.88. IR (ATR): $\nu(\text{CN}/\text{cm}^{-1}) = 1990$.

$[(\eta^5\text{-C}_5\text{Me}_5)\text{Ru}(\eta^3\text{-ebolnd})(\text{CN-o-Xy})]$ (7). Toluene was added to a mixture of 50 mg (0.13 mmol) of **3** and 17 mg (0.13 mmol) of 2,6-dimethylphenyl isocyanide. Full conversion of the starting materials was observed after 2 d at room temperature. The solvent was removed *in vacuo*. Recrystallization from a concentrated Et_2O solution at -30°C gave 39 mg (0.08 mmol, 58%) of yellow crystals. ^1H NMR (400 MHz; C_6D_6): δ 6.98 (dd, J_{HH} 1.5, 7.5 Hz, 1H, H10), 6.83 (t, J_{HH} 7.5 Hz, 1H, H7), 6.75 (t, 1H, phenyl), 6.74 (d, 2H, phenyl), 6.64 (dt, J_{HH} 1.4, 7.5 Hz, 1H, H9), 6.48 (dt, J_{HH} 1.5, 7.5 Hz, 1H, H8), 4.25 (d, J_{HH} 5.8 Hz, 1H, H3), 3.51 (dd, J_{HH} 5.8, 6.8 Hz, 1H, H2), 3.28 (dd, J_{HH} 1.3, 6.8 Hz, 1H, H1) 2.24 (s, 6H, $\text{C}_6\text{H}_4\text{-o-Me}_2$), 1.69 (s, 15H, C_5Me_5), 1.68 (s, 3H, CMe_2), 1.66 (s, 3H, CMe_2) ppm. ^{13}C NMR (100 MHz; C_6D_6): δ 145.5 (C4), 141.0 (C5), 134.6 (*ipso*-phenyl), 131.5 (*ipso*-C-NC), 127.6 (phenyl), 125.5 (phenyl), 125.2 (C7), 124.9 (C9), 123.9 (C10), 122.6 (C8), 91.0 (C_5Me_5), 71.3 (C2), 64.9 (C1), 53.6 (C3), 40.0 (C6), 38.3 (CMe_2), 31.0 (CMe_2), 19.2 ($\text{C}_6\text{H}_4\text{-o-Me}_2$), 10.3 (C_5Me_5) ppm. The signal for the isocyanide carbon could not be observed. Anal. Calcd for $\text{C}_{31}\text{H}_{37}\text{NRu}$: C, 70.96; H, 7.11; N, 2.67. Found: C, 71.01; H, 7.09; N, 2.63. IR (ATR): $\nu(\text{CN}/\text{cm}^{-1})$ 1955.

$[(\eta^5\text{-C}_5\text{Me}_5)\text{Ru}(\eta^3\text{-ebolnd})(\text{IME})]$ (8). C_6D_6 was added to a mixture of 50 mg (0.13 mmol) of **3** and 16 mg (0.13 mmol) of 1,3,4,5-tetramethylimidazol-2-ylidene. Full conversion of the starting materials was observed after 3 d at 60°C . The solvent was removed *in vacuo*, and the compound was precipitated from pentane/hexamethylidisiloxane at -30°C . This gave 51 mg (0.10 mmol, 78% yield) of a yellow solid. ^1H NMR (400 MHz; C_6D_6): δ 6.98 (dd, J_{HH} 1.5, 7.5 Hz, 1H, H10), 6.73 (dt, J_{HH} 1.5, 7.3 Hz, 1H, H9), 6.67 (dt, J_{HH} 1.5, 7.3 Hz, 1H, H8), 6.57 (dd, J_{HH} 1.5, 7.5 Hz, 1H, H7), 3.59 (s, 3H, NMe), 3.56 (d, J_{HH} 6.3 Hz, 1H, H3), 3.55 (dt, J_{HH} 1.8, 5.7 Hz, 1H, H2), 3.47 (s, 3H, NMe), 2.99 (dd, J_{HH} 1.7, 6.3 Hz, 1H, H1), 1.74 (s, 3H, H12), 1.55 (s, 15H, C_5Me_5), 1.51 (d, J_{HH} 0.8 Hz, 3H, CMe), 1.47 (d, J_{HH} 0.8 Hz,

3H, CMe), 1.15 (s, 3H, H11) ppm. ^{13}C NMR (100 MHz; C_6D_6): δ 194.1 (NCN), 147.5 (C4), 142.0 (C5), 125.5 (C10), 124.0 (CMe), 123.5 (C9), 123.3 (C7), 123.2 (CMe), 120.8 (C8), 85.7 (C_5Me_5), 67.3 (C2), 53.3 (C1), 46.2 (C3), 42.1 (C12), 39.3 (NMe), 39.2 (C6), 36.3 (NMe), 27.8 (C11), 10.1 (C_5Me_5), 9.7 (CMe), 9.4 (CMe) ppm. Anal. Calcd for $\text{C}_{29}\text{H}_{40}\text{N}_2\text{Ru}$: C, 67.28; H, 7.79; N, 5.41. Found: C, 67.36; H, 7.68; N, 5.35.

ASSOCIATED CONTENT

Supporting Information

Crystallographic information files (CIF), NMR spectra, the cyclovoltammetric data for **3**, and the crystal structure data for $[(\eta^5\text{-C}_5\text{Me}_5)\text{Ru}(\eta^3\text{-oInd}^{\text{Me}})(\text{CN-o-Xy})]$. This material is available free of charge via the Internet at <http://pubs.acs.org>.

AUTHOR INFORMATION

Notes

The authors declare no competing financial interest.

ACKNOWLEDGMENTS

We thank Dr. Andreas Glöckner for helpful discussions.

REFERENCES

- (1) (a) Ernst, R. D. *Acc. Chem. Res.* **1985**, *18*, 56–62. (b) Ernst, R. D. *Chem. Rev.* **1988**, *88*, 1255–1291. (c) Ernst, R. D. *Comments Inorg. Chem.* **1999**, *21*, 285–325.
- (2) (a) Bleeke, J. R. *Organometallics* **2005**, *24*, 5190–5207. (b) Paz-Sandoval, M. A.; Rangel-Salas, I. I. *Coord. Chem. Rev.* **2006**, *250*, 1071–1106.
- (3) (a) Glöckner, A.; Àrias, Ò.; Bannenberg, T.; Daniliuc, C. G.; Jones, P. G.; Tamm, M. *Dalton Trans.* **2011**, *40*, 11511–11518. (b) Glöckner, A.; Bannenberg, T.; Ibrom, K.; Daniliuc, C. G.; Freytag, M.; Jones, P. G.; Walter, M. D.; Tamm, M. *Organometallics* **2012**, *31*, 4480–4494.
- (4) (a) Rerek, M. E.; Ji, L.-N.; Basolo, F. *J. Chem. Soc., Chem. Commun.* **1983**, 1208–1209. (b) Rerek, M. E.; Basolo, F. *J. Am. Chem. Soc.* **1984**, *106*, 5908–5912. (c) O’Conner, J. M.; Casey, C. P. *Chem. Rev.* **1987**, *87*, 307–318. (d) Calhorda, M. J.; Veiros, L. F. *Coord. Chem. Rev.* **1999**, *185–186*, 37–51. (e) Cadierno, V.; Díez, J.; Pilar Gamasa, M.; Gimeno, J.; Lastra, E. *Coord. Chem. Rev.* **1999**, *193–195*, 147–205.
- (5) (a) Calhorda, M. J.; Romão, C. C.; Veiros, L. F. *Chem.—Eur. J.* **2002**, *8*, 868–875. (b) Veiros, L. F.; Calhorda, M. J. *Dalton Trans.* **2011**, *40*, 11138–11146.
- (6) (a) DiMauro, P. T.; Wolczanski, P. T. *Organometallics* **1987**, *6*, 1947–1954. (b) Basta, R.; Wilson, D. R.; Ma, H.; Arif, A. M.; Herber, R. H.; Ernst, R. D. *J. Organomet. Chem.* **2001**, *637–639*, 172–181. (c) LeSuer, R.; Basta, R.; Arif, A. M.; Geiger, W. E.; Ernst, R. D. *Organometallics* **2003**, *22*, 1487–1493.
- (7) (a) Feng, S.; Klosin, J.; Kruper, W. J.; McAdon, M. H.; Neithamer, D. R.; Nickias, P. N.; Patton, J. T.; Wilson, D. R.; Abboud, K. A.; Stern, C. L. *Organometallics* **1999**, *18*, 1159–1167. (b) Rajapakshe, A.; Gruhn, N. E.; Lichtenberger, D. L.; Basta, R.; Arif, A. M.; Ernst, R. D. *J. Am. Chem. Soc.* **2004**, *126*, 14105–14116. (c) Basta, R.; Arif, A. M.; Ernst, R. D. *Organometallics* **2005**, *24*, 3974–3981. (d) Rajapakshe, A.; Basta, R.; Arif, A. M.; Ernst, R. D.; Lichtenberger, D. L. *Organometallics* **2007**, *26*, 2867–2871.
- (8) (a) Winkhaus, G.; Pratt, L.; Wilkinson, G. *J. Chem. Soc.* **1961**, 3807–3813. (b) Henry, W. P.; Rieke, R. D. *J. Am. Chem. Soc.* **1983**, *105*, 6314–6316. (c) Leong, V. S.; Cooper, N. J. *Organometallics* **1988**, *7*, 2058–2060. (d) Thompson, R. L.; Lee, S.; Rheingold, A. L.; Cooper, N. J. *Organometallics* **1991**, *10*, 1657–1659. (e) Kündig, E. P.; Jeger, P.; Bernardinelli, G. *Angew. Chem., Int. Ed.* **1995**, *34*, 2161–2163. (f) Sun, S.; Dullaghan, C. A.; Carpenter, G. B.; Sweigart, D. A.; Lee, S. S.; Chung, Y. K. *Inorg. Chim. Acta* **1997**, *262*, 213–217. (g) Veauthier, J. M.; Chow, A.; Fraenkel, G.; Geib, S. J.; Cooper, N. J. *Organometallics* **2000**, *19*, 3942–3947. (h) Son, S. U.; Paik, S.-J.; Park,

- K. H.; Lee, Y.-A.; Lee, I. S.; Chung, Y. K. *Organometallics* **2002**, *21*, 239–242.
- (9) (a) Son, S. U.; Paik, S.-J.; Lee, I. S.; Lee, Y.-A.; Chung, Y. K.; Seok, W. K.; Lee, H. N. *Organometallics* **1999**, *18*, 4114–4118. (b) Georg, A.; Kreiter, C. G. *Eur. J. Inorg. Chem.* **1999**, 651–654. (c) Veiros, L. F. *Organometallics* **2000**, *19*, 31127–3136.
- (10) Arnold, R. T.; Buckley, J. S.; Richter, J. *J. Am. Chem. Soc.* **1947**, *69*, 2322–2325.
- (11) (a) Vebrel, J.; Carrié, R. *Bull. Soc. Chim. Fr.* **1982**, II–161. (b) Nagata, T.; Imagawa, K.; Yamada, T.; Makaiyama, T. *Bull. Chem. Soc. Jpn.* **1995**, *68*, 1455.
- (12) (a) Schlosser, M. *J. Organomet. Chem.* **1967**, *8*, 9–16. (b) Schlosser, M. *Pure Appl. Chem.* **1988**, *60*, 1627–1634.
- (13) (a) Bates, R. B.; Gosselink, D. W.; Kaczynski, J. A. *Tetrahedron Lett.* **1967**, *8*, 205–210. (b) Bates, R. B.; Brenner, S.; Cole, C. M.; Davidson, E. W.; Forsythe, G. D.; McCombs, D. A.; Roth, A. S. *J. Am. Chem. Soc.* **1973**, *95*, 926–927. (c) Olah, G. A.; Asensio, G.; Mayr, H.; Schleyer, P. v. R. *J. Am. Chem. Soc.* **1978**, *100*, 4347–4352. (d) Sustmann, R.; Dern, H.-J. *Chem. Ber.* **1983**, *116*, 2958–2971.
- (14) Elschenbroich, C.; Bilger, E.; Ernst, R. D.; Wilson, D. R.; Kralik, M. S. *Organometallics* **1985**, *4*, 2068–2071.
- (15) (a) Navarro, M. E.; Cházaro, L. F.; González, F. J.; Paz-Sandoval, M. A. *J. Electroanal. Chem.* **2000**, *480*, 18–25. (b) Cházaro-Ruiz, L. F.; González, F. J.; Paz-Sandoval, M. A. *J. Electroanal. Chem.* **2005**, *585*, 19–27. (c) Cházaro-Ruiz, L. F.; Maisonhaute, E.; Thouin, L.; Amatore, C.; González, F. J.; Paz-Sandoval, M. A. *J. Electroanal. Chem.* **2007**, *611*, 96–106.
- (16) (a) Bottrill, M.; Green, M.; O'Brien, E.; Smart, L. E.; Woodward, P. *J. Chem. Soc., Dalton Trans.* **1980**, 292–298. (b) Butler, I. R.; Cullen, W. R.; Lindsell, W. E.; Preston, P. N.; Rettig, S. J. *J. Chem. Soc., Chem. Commun.* **1987**, 439–441. (c) Zaworotko, M. J.; Sturge, K. C.; White, P. S. *J. Organomet. Chem.* **1990**, *389*, 333–340. (d) Müller, P.; Bernardinelli, G.; Motallebi, S. *Helv. Chim. Acta* **1990**, *73*, 1242–1249.
- (17) Hockett, S. C.; Angelici, R. J. *Organometallics* **1988**, *7*, 1491–1500.
- (18) (a) Bruce, M. I.; Catlow, A.; Cifuentes, M. P.; Snow, M. R.; Tiekink, E. R. T. *J. Organomet. Chem.* **1990**, *397*, 187–202. (b) Bruce, M. I.; Koutsantonis, G. A.; Tiekink, E. R. T.; Nicholson, B. K. *J. Organomet. Chem.* **1991**, *420*, 271–288. (c) Urbanos, F.; Halcrow, M. A.; Fernandez-Baeza, J.; Dahan, F.; Labroue, D.; Chaudret, B. *J. Am. Chem. Soc.* **1993**, *115*, 3484–3493. (d) Pigge, F. C.; Coniglio, J. J.; Rath, N. P. *Organometallics* **2005**, *24*, 5424–5430. (e) Pigge, F. C.; Dhanya, R.; Swenson, D. C. *Organometallics* **2009**, *28*, 3869–3875. (f) Chin, R. M.; Simonson, A.; Mauldin, J.; Criswell, J.; Brennessel, W. *Organometallics* **2010**, *29*, 3868–3875.
- (19) Alternatively, *supine* (= *exo*) and *prone* (= *endo*) can be used to distinguish the two orientations. See: Steinborn, D. *Grundlagen der Metallorganischen Komplexkatalyse, 1. Auflage*; B. D. Teubner Verlag: Wiesbaden, Germany, 2007.
- (20) (a) Lee, G. H.; Peng, S. M.; Lush, S. F.; Liao, M. Y.; Liu, R. S. *Organometallics* **1987**, *6*, 2094–2099. (b) Cheng, M.-H.; Wu, Y.-J.; Wang, S.-L.; Liu, R.-s. *J. Organomet. Chem.* **1989**, *373*, 119–127. (c) Iwata, M.; Okazaki, M.; Tobita, H. *Chem. Commun.* **2003**, 2744–2745.
- (21) (a) Crocker, M.; Green, M.; Morton, C. E.; Nagle, K. R.; Orpen, A. G. *J. Chem. Soc., Dalton Trans.* **1985**, 2145–2153. (b) Hsu, L. Y.; Nordman, C. E.; Gibson, D. H.; Hsu, W. L. *Organometallics* **1989**, *8*, 241–244. (c) Matsuo, Y.; Uematsu, T.; Nakamura, E. *Eur. J. Inorg. Chem.* **2007**, 2729–2733.
- (22) The X-ray crystal structure of $[(\eta^5\text{-C}_5\text{Me}_5)\text{Ru}(\eta^3\text{-oInd}^{\text{Me}})(\text{CN-o-Xy})]$ is presented in the Supporting Information.
- (23) Connelly, N. G.; Geiger, W. E. *Chem. Rev.* **1996**, *96*, 877–910.
- (24) Job, R.; Earl, R. *Inorg. Nucl. Lett.* **1979**, *15*, 81–83.
- (25) Kohl, F. X.; Jutzi, P. *J. Organomet. Chem.* **1983**, *243*, 119–121.
- (26) Fagan, P.; Ward, M. D.; Calabrese, J. C. *J. Am. Chem. Soc.* **1989**, *111*, 1689–1719.
- (27) Sheldrick, G. M. *Acta Crystallogr.* **2008**, *A64*, 112–122.